Article

Performance Characterization and Auto-Ignition Performance of a Rapid Compression Machine

Hao Liu, Hongguang Zhang *, Zhicheng Shi, Haitao Lu, Guangyao Zhao and Baofeng Yao

College of Environmental and Energy Engineering, Beijing University of Technology, Pingleyuan No.100, Beijing 100124, China; E-Mails: liuhao_0225@163.com (H.L.); 15933731855@163.com (Z.S.); 13641375795@163.com (H.L.); zhaoguangyao105@163.com (G.Z.); yaobf@bjut.edu.cn (B.Y.)

* Author to whom correspondence should be addressed; E-Mail: zhanghongguang@bjut.edu.cn; Tel.: +86-10-6739-2469; Fax: +86-10-6739-2774.

Abstract: A rapid compression machine (RCM) test bench is developed in this study. The performance characterization and auto-ignition performance tests are conducted at an initial temperature of 293 K, a compression ratio of 9.5 to 16.5, a compressed temperature of 650 K to 850 K, a driving gas pressure range of 0.25 MPa to 0.7 MPa, an initial pressure of 0.04 MPa to 0.09 MPa, and a nitrogen dilution ratio of 35% to 65%. A new type of hydraulic piston is used to address the problem in which the hydraulic buffer adversely affects the rapid compression process. Auto-ignition performance tests of the RCM are then performed using a DME–O_2–N_2 mixture. The two-stage ignition delay and negative temperature coefficient (NTC) behavior of the mixture are observed. The effects of driving gas pressure, compression ratio, initial pressure, and nitrogen dilution ratio on the two-stage ignition delay are investigated. Results show that both the first-stage and overall ignition delays tend to increase with increasing driving gas pressure. The driving gas pressure within a certain range does not significantly influence the compressed pressure. With increasing compression ratio, the first-stage ignition delay is shortened, whereas the second-stage ignition delay is extended. With increasing initial pressure, both the first-stage and second-stage ignition delays are shortened. The second-stage ignition delay is shortened to a greater extent than that of the first-stage. With increasing nitrogen dilution ratio, the first-stage ignition delay is shortened, whereas the second-stage is extended. Thus, overall ignition delay presents different trends under various compression ratios and compressed pressure conditions.

1. Introduction

The increasingly serious energy crisis and environmental problems have lead to the pollution emissions of internal combustion (IC) engines to gain considerable attention. Methods to improve the combustion thermal efficiency and reduce the emissions of IC engines have become the focus of many scholars. To gain a better understanding of the ignition and combustion characteristics of various types of fuels, scholars around the world have developed various experimental devices, such as a constant volume combustion bomb, shock tube, single cylinder test engine, and rapid compression machine (RCM).

A detailed understanding of combustion kinetics is important to address practical combustion problems. The ignition delay time of fuels is one of the significant parameters for the combustion optimization of IC engines. For homogeneous charge compression ignition (HCCI) or other new combustion modes, ignition delay time is also a crucial parameter. There are some experimental data and empirical formulas for the ignition delay time of conventional fuels, but for most of the IC engine alternative fuels, substantial and detailed research work is still required.

In the study of ignition delay time, RCM and shock tube are two of the most widely used facilities. RCM simulates the process of adiabatic compression and ignition and gives a direct way of measuring the ignition delay. Compared with shock tubes, RCM is used to study the auto-ignition characteristics of fuels in the temperature range of low to intermediate, while the shock tube is used to study auto-ignition characteristics of gas mixtures at a higher temperature and pressure than those of RCM. The experimental data from RCM or shock tube could complement each other well. In literature [1], the similarities and differences of experimental results between RCM and shock tube are studied.

According to the purposes of practical research, RCMs present a variety of structures.

RCMs [2–14] and rapid compression and expansion machines (RCEMs) [15–19] can be classified on the basis of whether they can perform an expansion stroke. The distinguishing characteristic of RCM from RCEM is that when the piston of the RCM moves to the top dead center (TDC), the piston gets locked (including driving gas pressure locking or mechanical locking) without an expansion process, such that a constant volume combustion chamber is formed.

As regards to the structural arrangement, RCM can be classified into the single axial compression type or opposed compression type [5,19]. Most RCMs adopt single axial compression, which is similar to the compression stroke of IC engine pistons. The opposed compression type can offer a faster compression speed (approximately twice that of single axial compression type) with the same compression ratio because of drive and compression processes on two sides. Furthermore, the single axial compression RCM includes horizontal, vertical [13], and right-angled types [11,12,16]. The horizontal types are the most commonly used pattern, the vertical type considers a certain movement direction of the piston, and most right-angled types are used in a situation in which the piston motion is conducted by a cam.

As regards to the different driving methods, RCM uses potential energy drive, motor drive [8,15], and pneumatic drive types [6,7]. For enhanced effect and convenience, an increasing number of RCMs use the pneumatic drive type. Several RCMs use the motor drive type. Although the potential energy drive is an old method, the piston is driven by the potential energy of a falling cam in some cases [16].

As regards to the brake mode, RCM uses a hydraulic [2–4] or mechanical brake. The mechanical brake includes various forms, such as mechanical arm [9,10], mechanical absorber [7], and cam [11,12,16].

Finally, as regards to the transmission mode, RCMs can be classified into linear connecting rod [2–4], free-piston [14,19], and crankshaft and connecting rod types [15,17].

For the study of chemical reaction kinetics, the experimental data obtained from RCM can facilitate the understanding of as well as verify and improve the detailed chemical reaction mechanism of fuels.

An RCM is developed in this study. Performance characterization and auto-ignition performance tests are conducted. In the performance characterization tests, a novel hydraulic piston is used to address the problem wherein the hydraulic buffer adversely affects the rapid compression process. By using auto-ignition performance tests, the influences of driving pressure, compression ratio (compressed temperature), and initial pressure (compressed pressure) on the two-stage ignition delay of the DME–O_2–N_2 mixture are investigated.

2. Description of the RCM

2.1. Configuration of the RCM

Figure 1 shows the schematic diagram of the RCM test bench used in this study.

Figure 1. Schematic diagram of the rapid compression machine (RCM) test bench. 1. Quartz window; 2. Gas inlet/outlet ports; 3. Pressure transducer; 4. Reactor cylinder; 5. Creviced piston; 6. Clearance spacers; 7. Hydraulic cylinder; 8. Hydraulic piston with T-shaped channel; 9. Stroke spacers; 10. Driver cylinder.
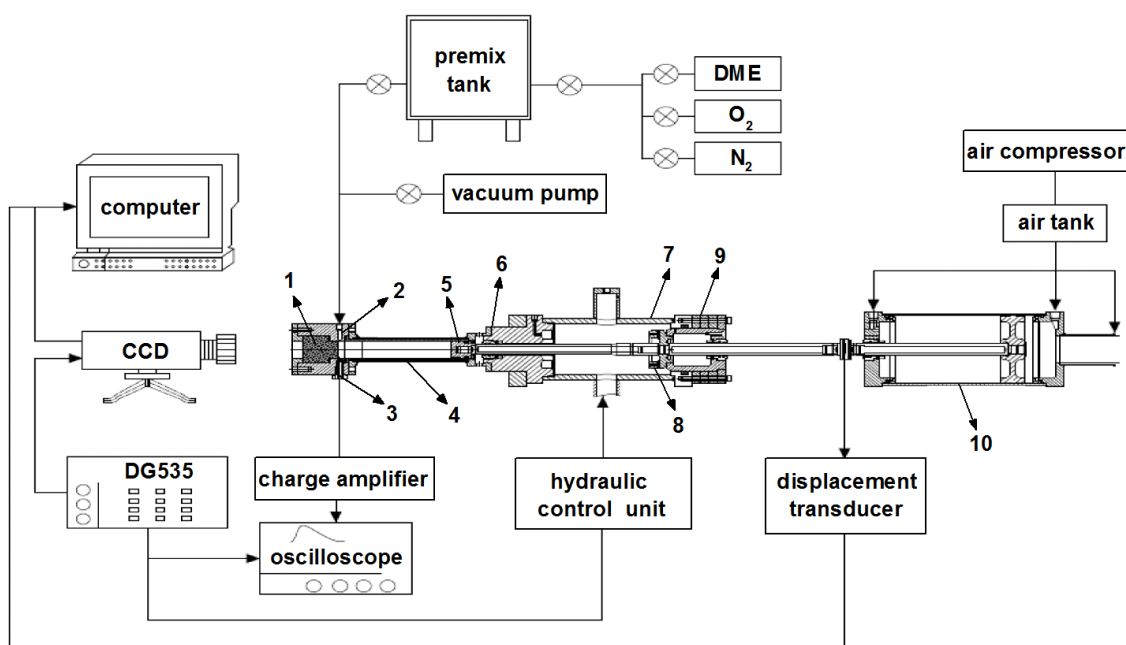
The RCM is the main part of the test bench and consists of the driver, hydraulic, and reactor cylinders. The overall structure is horizontal, and the driver piston, reactor piston, and hydraulic piston are connected by the linear connecting rod. The piston and connecting rod assembly propelled by driving gas pressure moves with a high speed from bottom dead center (BDC) to TDC and gets locked in the final position of TDC, creating a constant volume chamber. The reactive mixture filled in the reactor cylinder before the compression process is initially compressed and then ignites in a very short time.

The stroke of the piston and connecting rod assembly can be changed by adjusting stroke spacers (the thickness of each piece is 20 mm, a total of three pieces) mounted on the rear portion of the hydraulic cylinder. The position of the BDC can be adjusted by changing the number of stroke spacers between the rear cover and hydraulic cylinder body; hence, the compression stroke can vary from 190 to 250 mm. A constant volume chamber can be formed when the reactor piston reaches the TDC, the length of which can range from 12 to 20 mm by adjusting the number of the clearance spacers (the thickness of each piece is from 1 to 2 mm). These spacers are installed between the front side of the hydraulic cylinder and the rear portion of the reactor cylinder.

The main parameters of the RCM are listed in Table 1.

Table 1. Main parameters of the rapid compression machine (RCM).

Item	Parameter
Stroke	190 mm to 250 mm
Length of constant volume chamber	12 mm to 20 mm
Reactor cylinder bore	50 mm
Compression ratio	8.42 to 16.9
Average piston motion speed	9 m/s

2.2. Operation Principle of the RCM Test Bench

The RCM test bench includes the pneumatic drive, hydraulic control, reactor cylinder, gas supply, and data acquisition systems (Figure 1).

The pneumatic drive system mainly includes the air compressor, air tank, and driver cylinder. The air tank and the driver cylinder are directly connected by a pipeline with a bore of DN80, and a butterfly valve is used for on-off control. The hydraulic control system, which is made up of a hydraulic control unit and a hydraulic cylinder, controls a series of actions such as the start, buffer, and brake of the piston. The reactor cylinder mainly includes the cylinder body, cylinder head, quartz window, and reactor piston. The gas supply system mainly includes the experimental gas, premix tank, and vacuum pump. The data acquisition system mainly includes the Kistler 6125C pressure transducer, Kistler 5011 charge amplifier, Tektronix MS04000 oscilloscope, displacement transducer, high speed camera, computer, and DG535 synchronization signal generator.

Air is filled into the air tank to a certain pressure by air compressor. To ensure the reproducibility of the experiment, the formation of the mixture gas is carefully considered. The reactive mixtures are set to a certain equivalence ratio or blending ratio and stirred at least 30 min in the premix tank. A pressure transmitter is used to display the pressure data after each experimental gas is filled into the premix tank, and the pressure of 0.2 or 0.3 MPa will be obtained in the premix tank after finishing the

gas charging process. Since the volume of the premix tank is much bigger than that of reactor chamber, mixtures in the premix tank can provide many experiments.

Before the experiment, when the piston and connecting rod assembly is at the BDC, a sealed cavity is formed by the rear portion of hydraulic piston and the rear cover of the hydraulic cylinder. Next, the hydraulic cylinder is filled with hydraulic oil with the pressure of 6 MPa in the front side of hydraulic piston by the hydraulic control unit. The hydraulic piston has a bore of 110 mm. The ratio between the piston areas is 3.3 pneumatic to hydraulic, but the ratio between the pressures is at least 8.5 hydraulic to pneumatic. Therefore, the hydraulic braking force can be higher than the drive gas force in the driver cylinder; hence, the piston and connecting rod assembly is locked at BDC and cannot moved forward.

At the beginning of the experiment, the butterfly valve between the air tank and the driver cylinder is switched on. A series of actions such as hydraulic oil releasing, oscilloscope triggering, and the shooting of a high speed camera are controlled by a DG535 synchronization signal generator. When the hydraulic oil inside the hydraulic cylinder is rapidly released by the hydraulic control unit, the hydraulic oil in front of the hydraulic piston rushes into the rear portion of hydraulic piston via the clearance, given that a certain clearance exists between the hydraulic piston and the cylinder wall. Hence, when the piston and the connecting rod assembly move forward, the influence of the hydraulic system on the piston and connecting rod movement is suppressed to a minimum during the rapid compression process. Finally, the piston and connecting rod assembly decelerates by means of a hydraulic buffer and gets locked when the piston reaches the TDC.

During the experiment, the pressure of the reactive mixtures is obtained using the Kistler 6125C pressure transducer and Kistler 5011 charge amplifier (Winterthur, Switzerland). The pressure data are recorded by a Tektronix MS04000 oscilloscope (Beaverton, OR, USA).

A hydraulic piston with a special structure is designed with the purpose of flexibly adjusting the hydraulic buffer to obtain a better hydraulic buffer effect (Figures 2 and 3).

Six groups of T-shaped channels exist on the top of the piston (solid box A in Figure 2). The hydraulic buffer effect can be adjusted by regulating the opening degree of the T-shaped channels. The slope (solid box B in Figure 2) and the hydraulic cylinder rear cover a sealed cavity when the hydraulic piston is at the BDC, which results in a better starting effect when the piston and connecting rod assembly start to move forward.

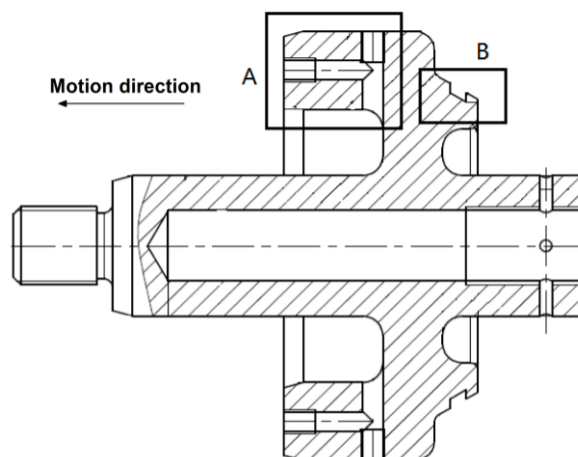**Figure 2.** Structure of hydraulic piston with T-shaped channels.

Figure 3. Hydraulic piston with T-shaped channels.

The reactor piston of the RCM used in this study adopts a "creviced piston" mentioned in reference [2]. A rolled-up vortex is observed at the piston face and the cylinder-wall interface when the conventional flat-top piston rapidly moves up. The structure of the creviced piston can reduce the influence of the rolled-up vortex on the "adiabatic core" in the reactor chamber at the end of compression process.

Furthermore, a few through-holes such as gas inlet/outlet ports and the installing hole of pressure transducer have been carefully considered to minimize the proportion accounting for the total clearance volume at the end of the compression as far as possible.

3. Performance Characterization Tests of the RCM

During the performance tests of the RCM, nitrogen is used as the charge in the reactor cylinder of the RCM. The pressure trace of the nitrogen in the reactor cylinder is shown in Figure 4. The initial pressure of nitrogen is 0.13 MPa, the initial temperature of nitrogen is 293 K (in this paper, the initial temperature is kept at 293 K for all the test conditions), the driving gas pressure in the driver cylinder is 0.6 MPa, and the compression ratio of the reactor cylinder is 13.6. The time point when the piston moves to the end of the compression stroke is taken as time zero. When the reactor piston reaches TDC and the compression pressure reaches the peak value, the pressure trace can be divided into three parts: rapid compression process, hydraulic buffer process, and pressure drop because of heat loss. During the rapid compression process, oil in front of hydraulic piston is released from the clearance between the piston and cylinder wall and the piston assembly (mainly including the reactor piston, the hydraulic piston, and the driver piston) rapidly moves forward, which lasts over 30 ms. During the hydraulic buffer process, the motion speed of the piston assembly is sharply lowered and the nitrogen pressure slowly rises. When the reactor piston moves to TDC, the piston assembly stops and gets locked.

The reactor piston moves from BDC to TDC in approximately 60 ms because of the high motion speed of the piston. The heat transfer between the nitrogen and cylinder wall is assumed to be zero, and the rapid compression process is assumed to be adiabatic (Figure 4). Based on the pressure trace (Figure 4), the volume variation of nitrogen during the compression process can be obtained (Figure 5). At the beginning of the hydraulic buffer process, the reactor piston is close to TDC. At the end of the hydraulic buffer process, the reactor piston reaches TDC. Compared with the rapid compression process for the hydraulic buffer process, although the volume variation of nitrogen is smaller,

the excessive hydraulic buffer results in a longer duration of the process (nearly 30 ms) which covers approximately half of the motion time of the piston assembly. This phenomenon has negative effects on measuring the ignition delay time. Furthermore, the compression pressure of nitrogen in the reactor cylinder will be more sensitive to the driving gas pressure in the driver cylinder.

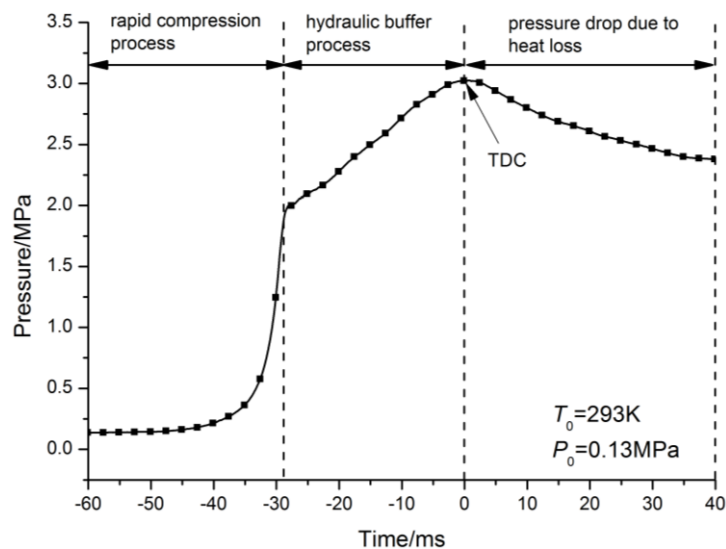**Figure 4.** Typical pressure trace of nitrogen in the RCM (before modification of the hydraulic buffer).
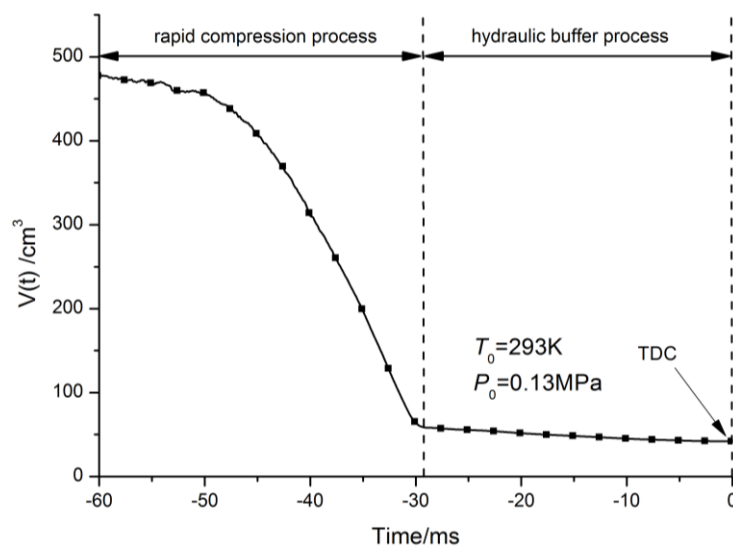

Figure 5. Volume variation of nitrogen in the RCM (before modification of the hydraulic buffer).


Considering the excessive hydraulic buffer, effects of the driving gas pressure on the compression pressure of nitrogen when the driving gas pressure ranges from 0.3 to 0.7 MPa are shown in Figure 6. With decreasing driving gas pressure, the compressed pressure of nitrogen decreases and the duration of the hydraulic buffer process increases. Therefore, the hydraulic buffer has a key effect on the operating performance of the RCM. Moreover, the hydraulic buffer should be modified to optimize the operating performance of the RCM. In addition, the compressed pressure of nitrogen in the reactor cylinder should be insensitive to the driving gas pressure in the driver cylinder.

Figure 6. Effect of driving gas pressure on the compression pressure (before modification of the hydraulic buffer).
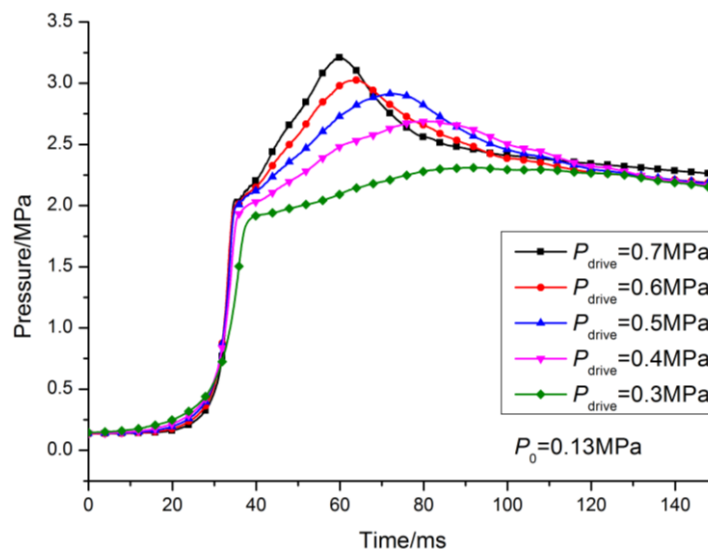

During the above-mentioned tests, all the T-shaped channels on the hydraulic piston (Figure 2) are absolutely closed to ensure that the RCM operates safely and smoothly. Based on the above analysis, the opening degree of a few T-shaped channels on the hydraulic piston is adjusted to modify the effect of the hydraulic buffer. Figure 7 shows the effect of the modification of the hydraulic buffer. The initial pressure of nitrogen is 0.13 MPa, the driving gas pressures in the driver cylinder are 0.65 MPa (before modification of the hydraulic buffer) and 0.5 MPa (after modification of the hydraulic buffer), respectively, the compression ratio of the reactor cylinder is kept at 13.6 MPa. As shown in Figure 7, given the modification of the hydraulic buffer, the duration of the hydraulic buffer process obviously decreases (less than 15 ms) and the peak value of the compression pressure (compressed pressure) of nitrogen increases.

Figure 7. Effect of modification of the hydraulic buffer.
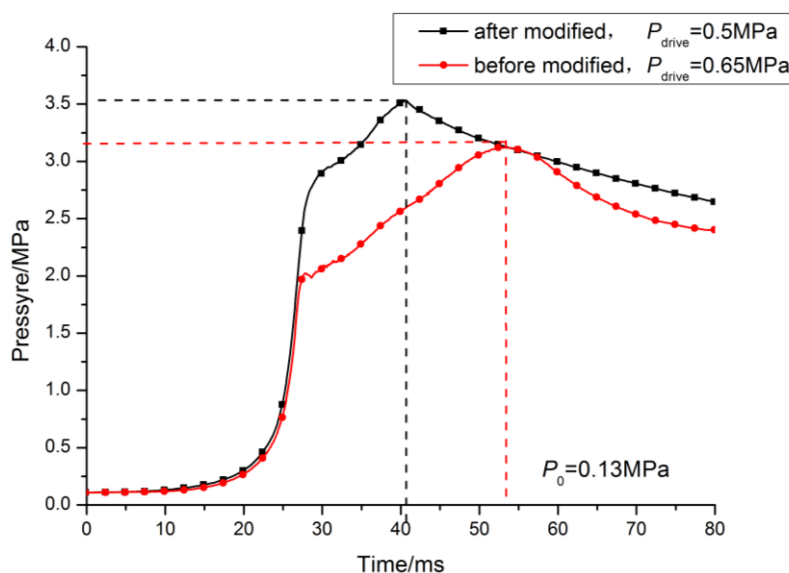
Although modification of the hydraulic buffer is obviously beneficial to decrease the duration of the hydraulic buffer process, absolute elimination of the hydraulic buffer process is unacceptable. As shown in Figure 8, at first, the oil in the hydraulic cylinder is discharged completely to eliminate the hydraulic buffer effect, and the piston assembly is then driven forward by the driver cylinder with a driving gas pressure of 0.2 MPa. When the hydraulic piston reaches its TDC (the reactor piston reaches its TDC), the hydraulic piston directly hits the front cover of the hydraulic cylinder. This phenomenon leads to serious vibrations of the RCM and even causes the reactor piston to instantaneously move backward, unable to stop, and immediately get locked (dashed box in Figure 8). Consequently, elimination of hydraulic buffer process has a negative effect on measuring the ignition delay time. Based on the above analysis, an appropriate hydraulic buffer process is needed to ensure that the optimal test results can be obtained.

Figure 8. Typical pressure trace of nitrogen in the RCM without hydraulic buffer.
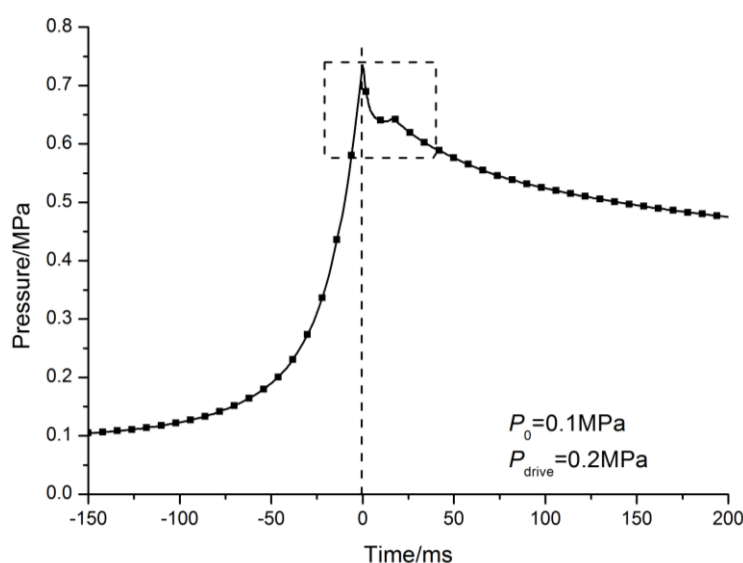
After modification of the hydraulic buffer, the effect of the driving gas pressure on the compression pressure of nitrogen with the compression ratio of 16.9 and the driving gas pressure ranging from 0.3 to 0.7 MPa is shown in Figure 9. The compressed pressure of nitrogen in the reactor cylinder is insensitive to the driving gas pressure (dashed box a in Figure 9). When the driving gas pressure in the driver cylinder is high, the compression pressure of nitrogen sharply rises (dashed box b in Figure 9). The duration of the compression process decreases to 20–30 ms, and the average motion speed of the reactor piston is about 9 m/s during the compression process.

With a driving gas pressure of 0.6 MPa in the driver cylinder and an initial pressure of nitrogen of 0.1 MPa, eight experiments are conducted and compared under the same conditions to ensure the reproducibility of tests under reactive conditions. Figure 10 demonstrates such a comparison by overlapping pressure traces of the eight tests for nitrogen. All the pressure traces closely follow each other, the highly repeatable test conditions can be obtained by the RCM designed in this study, and the RCM can meet the demands of auto-ignition performance tests (Figure 10).

Figure 9. Effect of driving gas pressure on the compression pressure (after modification of the hydraulic buffer).
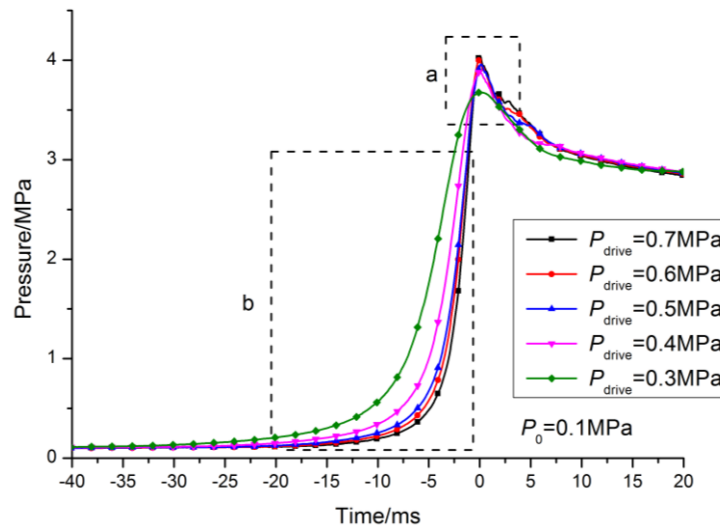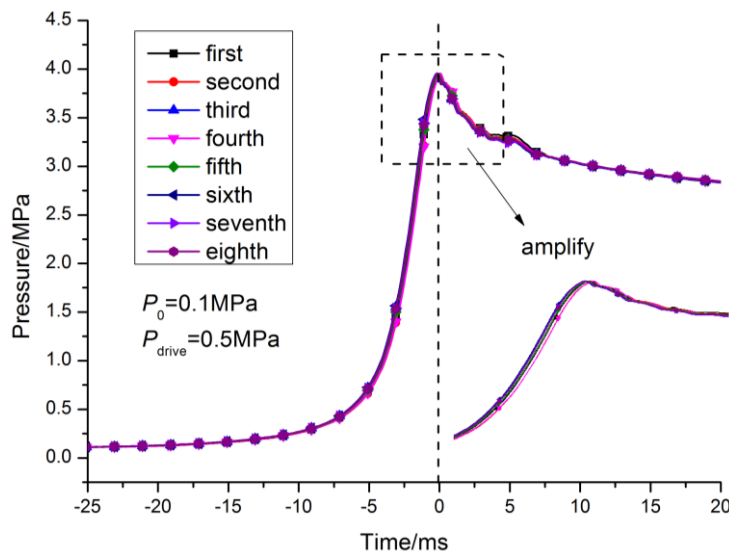

Figure 10. Demonstration of experimental repeatability for nitrogen.


4. Auto-Ignition Performance Tests of the RCM

The influence factors on the ignition delay of mixtures mainly include five aspects (Figure 11): (1) Blending ratio of mixture. Different kinds of fuels can be mixed in a certain proportion, such as dimethyl ether blending with hydrogen [20] and n-heptane blending with butanol [21], or diluting the mixture with inert gas [22], such as N_2, Ar, and CO_2; (2) Equivalence ratio of mixture. It can be divided into a fuel-air equivalence ratio and a fuel-oxygen equivalence ratio. In certain studies that involved the combustion emissions, the differences between oxygenated and non-oxygenated fuels should be considered when calculating the fuel-oxygen equivalence ratio; (3) Compressed pressure of mixture. With the change of compression, blending, and equivalence ratios, the desired compressed pressure can be achieved by adjusting the initial pressure of the mixture; (4) Compressed temperature of mixture. The compressed temperature can be adjusted by changing the compression ratio or initial

temperature of the mixture; (5) Turbulence. Some studies show that turbulence can play a substantial role in affecting the ignition delay [23].

Figure 11. The influence factors of ignition delay time.
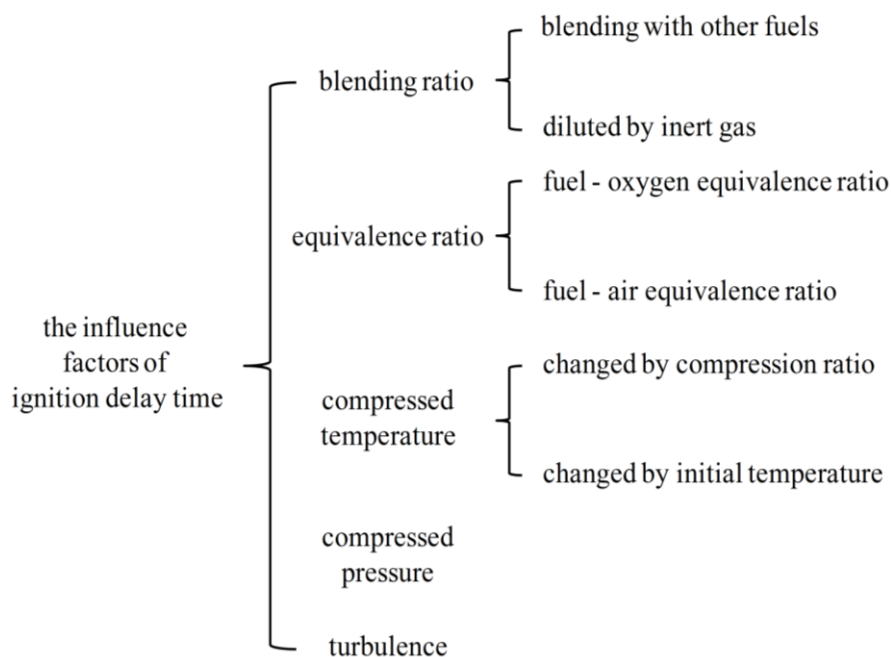
After the rapid compression process, the compressed temperature T_c in the reactor cylinder can be calculated using the following equation:

$$\int_{T_0}^{T_c} \frac{\gamma}{\gamma - 1} \frac{dT}{T} = \ln(\frac{P_c}{P_0}) \tag{1}$$

where T_0 and P_0 are initial temperature and initial pressure, respectively, at the beginning of compression; and γ is the ratio of specific heat of the mixture. The compressed temperature T_c is determined by compressed pressure P_c, which is the actual pressure at TDC and measured by pressure transducer.

Dimethyl ether (DME) can be produced from coal and natural gas at a relatively low cost. Since DME has high cetane number, oxygen content and vaporization heat, it has become a more promising alternative fuel. In view of the internal combustion engine applications, it is essential to study the combustion characteristics of DME, because it is helpful to improve the power and economic performances of the internal combustion engine.

In recent years, many scholars have studied the combustion characteristics of DME by using RCMs [24,25] or shock tubes [20,26]. Due to a low auto-ignition temperature, DME is an ideal fuel for compression ignition. In order to verify the auto-ignition performance tests of the RCM, DME is selected as the research object. DME–O_2–N_2 mixture is provided to study the effects of the driving gas pressure, compression ratio, initial pressure, and nitrogen dilution ratio on the two-stage ignition delay.

The related test conditions are shown in Table 2.

Table 2. Test conditions.

DME:O_2:N_2 (mole proportion)	Dilution ratio (%)	Driving gas pressure (MPa)	Compression ratio	Initial pressure (MPa)
1:3:20	36.31			
1:3:25	47.29			
1:3:30	55.04	0.25 to 0.6	9.5 to 16.5	0.04 to 0.09
1:3:35	60.81			
1:4:30	42.72			

4.1. Definition of Ignition Delay Time and Repeatability of Experiments

Dimethyl ether has a high cetane number, which results in an obvious two-stage combustion and two-stage ignition delay. In this study, the time point when the reactor piston moves to the TDC is taken as time zero. The first-stage ignition delay (τ_1 as shown in Figure 12) is defined as the time between the end of compression and the instant of first peak of pressure rising rate. The second-stage ignition delay (τ_2 as shown in Figure 12) is defined as the time from the instant of first peak of pressure rising rate to the instant of the rapid rise in pressure. With a compression ratio of 10.99, an initial pressure of 0.08 MPa, and a DME:O_2:N_2 = 1:3:30, the auto-ignition pressure of DME–O_2–N_2 mixture has an obvious two-stage ignition delay, and the overall ignition delay time τ is the sum of τ_1 and τ_2 (Figure 12). With the compression ratio of 16.43, the initial pressure of 0.04 MPa, and DME:O_2:N_2 = 1:4:30, the high compressed temperature makes the first-stage ignition delay disappear and the overall ignition delay time τ equal to τ_2 because of the high compression ratio (Figure 13).

Tests under the same conditions are conducted three to five times to ensure the accuracy of test results. According to the different test conditions, test results shown in Figure 14 are divided into three groups, the pressure traces for each group show a good consistency. It can be concluded that the repeatability of the auto-ignition test in this study can be ensured.

Figure 12. Definition of ignition delay time (ε = 10.99, P_0 = 0.08 MPa, DME:O_2:N_2 = 1:3:30).
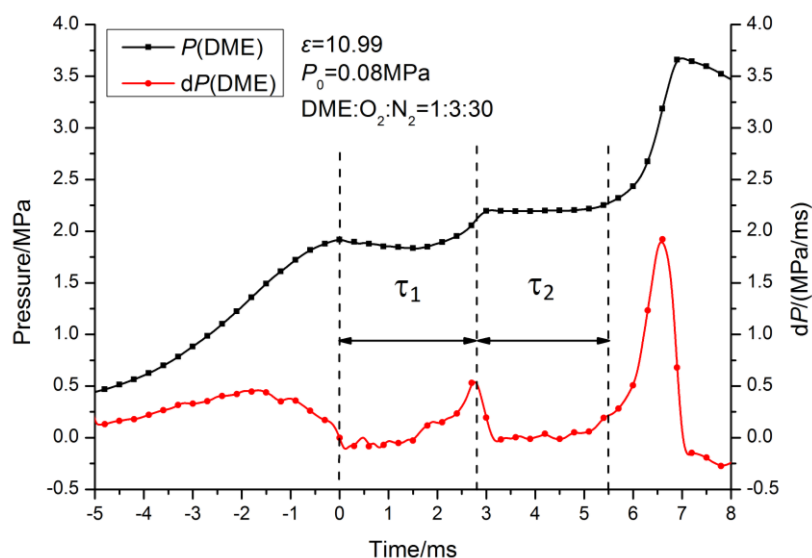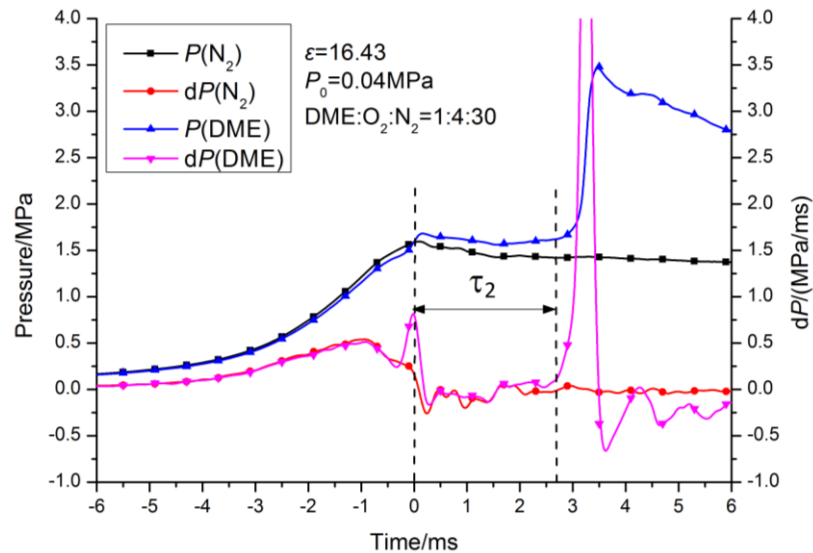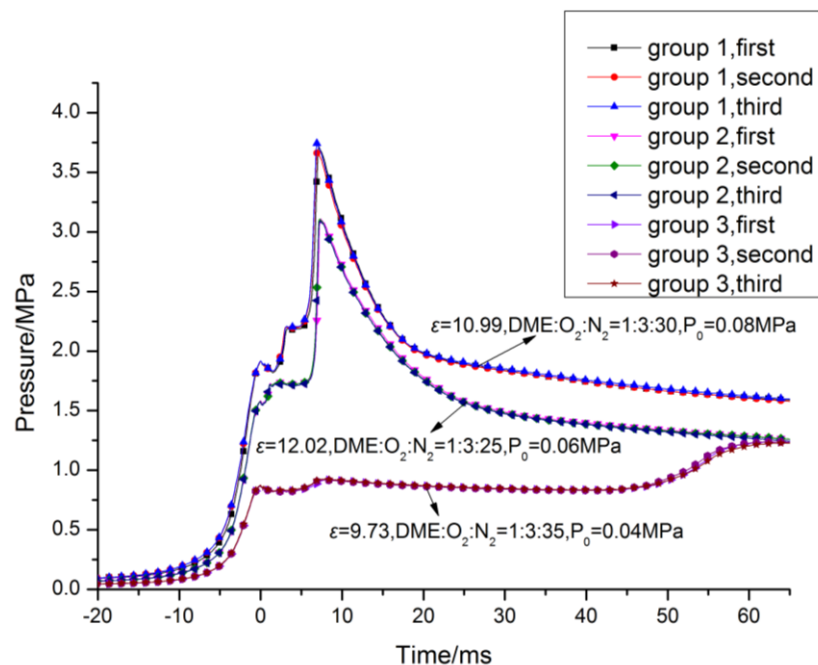
Figure 13. Definition of ignition delay time (ε = 16.43, P$_0$ = 0.04MPa, DME:O$_2$:N$_2$ = 1:4:30).

**Figure 14.** Experimental repeatability of compression and auto-ignition process.

4.2. Effect of Driving Gas Pressure on Two-Stage Ignition Delay

Figure 15 presents the effect of different driving gas pressures (0.25 to 0.6 MPa) on the ignition delay of the DME–O$_2$–N$_2$ mixture with a compression ratio of 10.99 and an initial pressure of 0.08 MPa. Both the first-stage and the overall ignition delays tend to increase with increasing driving gas pressure, which is opposite to the result of reference [27]. Two factors may contribute to this result. First, different from reference [27], the pressure fluctuation at the TDC is smaller in this study. Hence, the driving gas pressure within a certain range insignificantly influences the compressed pressure. Second, the DME–O$_2$–N$_2$ mixture is adopted in this study, which has a lower auto-ignition temperature than that of the NG–O$_2$–Ar mixture used in reference [27]. Because of the low piston

motion speed, the DME–O$_2$–N$_2$ mixture is much more influenced by compression time than the NG–O$_2$–Ar mixture. With a driving gas pressure of 0.25 MPa (Figure 17), the DME–O$_2$–N$_2$ mixture does not show any obvious first-stage ignition delay, which suggests that the mixture reaches the auto-ignition temperature during the rapid compression process. However, with a high driving gas pressure, the DME–O$_2$–N$_2$ mixture is less influenced by compression time; hence, both the first-stage and the overall ignition delays should be slightly extended.

Based on the above analysis, the driving gas pressure of 0.6 MPa is adopted in the following.

Figure 15. Effect of driving gas pressure on two-stage ignition delay.
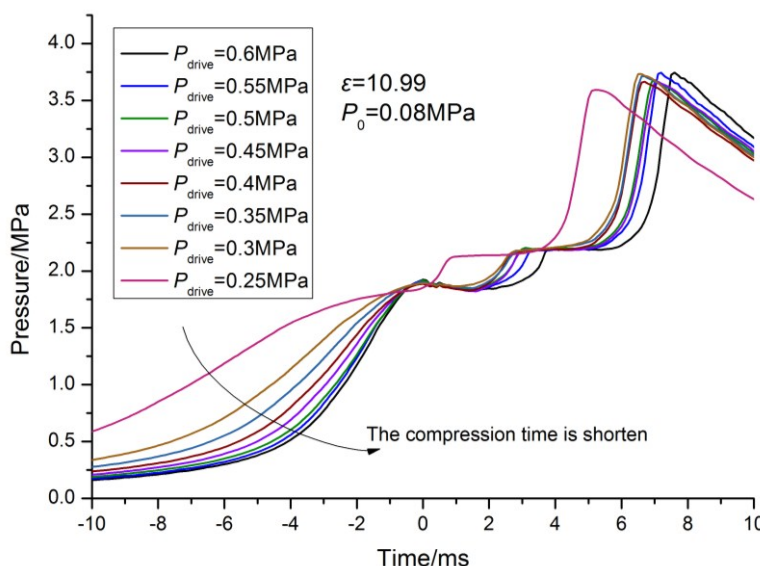
4.3. Effect of Compression Ratio on Two-Stage Ignition Delay

The changes in the two-stage ignition delay of the DME-O$_2$-N$_2$mixture are attributed to the combined result of compression ratio, initial pressure, and nitrogen dilution ratio. Figure 16 shows the changes of the two-stage ignition delay of the DME–O$_2$–N$_2$ mixture under the compression ratio of 9.73, 10.99, and 12.02 using a fixed mole proportion of DME:O$_2$:N$_2$ = 1:3:30 and DME:O$_2$:N$_2$ = 1:3:35 (P_0 = 0.08 MPa and 0.04 MPa, respectively). With rising compression ratio, the compressed pressure and compressed temperature of DME–O$_2$–N$_2$ mixture gradually increase and the first-stage ignition delay is gradually shortened, whereas the second-stage ignition delay is gradually extended (Figure 16). Under the compression ratio of 12.02 (Figure 16d), the excessively long second-stage ignition delay and excess heat loss lead to insufficient combustion. Regarding the changing trend of the overall ignition delay, the test results on the influence of compression ratio on the two-stage ignition delay of the DME–O$_2$–N$_2$ mixture are summarized in three groups, which are listed in Table 3. The DME–O$_2$–N$_2$ mixture overall ignition delay initially shortens and then extends with rising compression ratio under test condition group III. Under the test condition group II, the overall ignition delay gradually extends with rising compression ratio. The above-mentioned results show the negative temperature coefficient (NTC) behavior of the overall ignition delay of the DME–O$_2$–N$_2$ mixture. However, under test condition group I, the overall ignition delay shortens with

increasing compression ratio. Based on the above analysis, the NTC region of the overall ignition delay of the DME–O$_2$–N$_2$ mixture changes with nitrogen dilution ratios and compressed pressures.

Figure 16. Effect of compression ratio on two-stage ignition delay: (**a**) 55.04% dilution, $P_0 = 0.08$ MPa; (**b**) 55.04% dilution, $P_0 = 0.04$ MPa; (**c**) 60.81% dilution, $P_0 = 0.08$ MPa; and (**d**) 60.81% dilution, $P_0 = 0.04$ MPa.
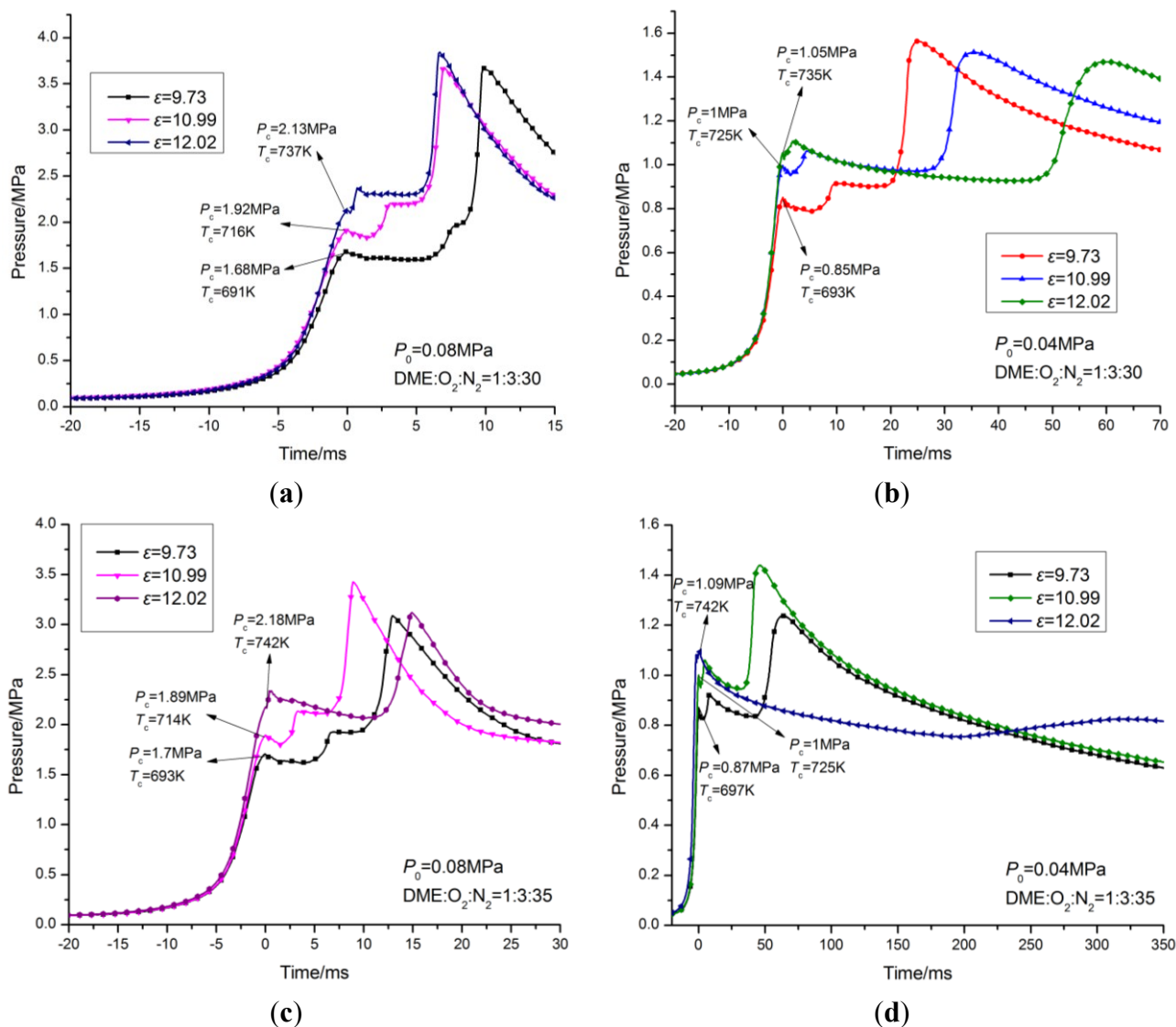

(**a**)   (**b**)   (**c**)   (**d**)

Table 3. Overall ignition delay changing trends with increasing compression ratio.

Test condition group	Test condition	Changing trend
I	55.04% dilution, $P_0 = 0.08$ MPa	Gradually shortens
II	55.04% dilution, $P_0 = 0.04$ MPa	Gradually extends
III	60.81% dilution, $P_0 = 0.04$ MPa 60.81% dilution, $P_0 = 0.08$ MPa	Initially shortens and then extends

4.4. Effect of Initial Pressure on Two-Stage Ignition Delay

Figure 17 shows the results of the DME–O$_2$–N$_2$ mixture auto-ignition performance test with the compression ratio of 13.83 and various initial pressures (0.03 to 0.08 MPa). The compressed

temperature under this compression ratio is calculated to be approximately 762 K. By contrast, Figure 18 shows the results of the DME–O_2–N_2 mixture auto-ignition performance test with the compression ratio of 10.99 and various initial pressures (0.04 to 0.09 MPa). The compressed temperature under this compression ratio is calculated to be approximately 715 K. The compressed pressure gradually increases with rising initial pressure (Figures 17 and 18). When the compressed pressure increases, both the first-stage and the second-stage ignition delays shorten. The second-stage ignition delay shortens to a greater extent than that of the first-stage. Under the compression ratio of 10.99, the first-stage ignition delay is long, whereas the second-stage ignition delay is short. Under the compression ratio of 13.83, the first-stage ignition delay is shorter compared to the second-stage ignition delay. Compared with the first-stage ignition delay, the second-stage ignition delay is much more strongly influenced by the compressed pressure. This phenomenon causes the overall ignition delay of the DME–O_2–N_2 mixture to shorten to a great extent with a high compression ratio when the initial pressure increases.

Figure 17. Effect of initial pressure on two-stage ignition delay ($\varepsilon = 13.83$).
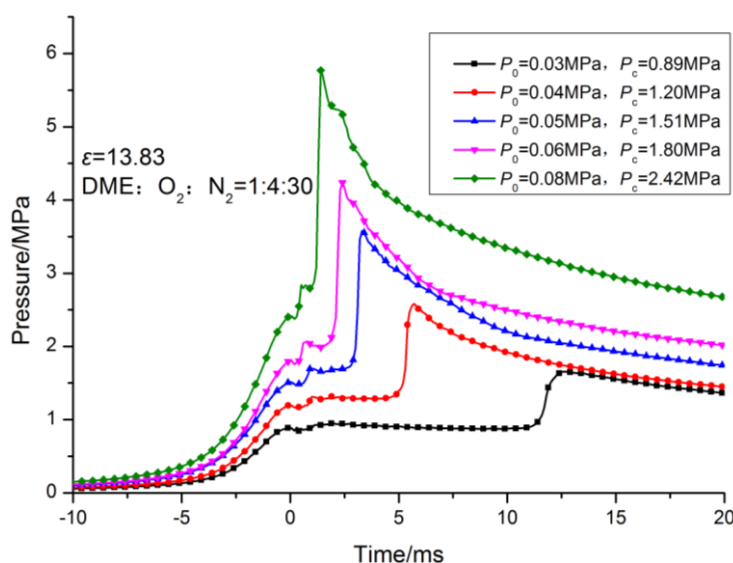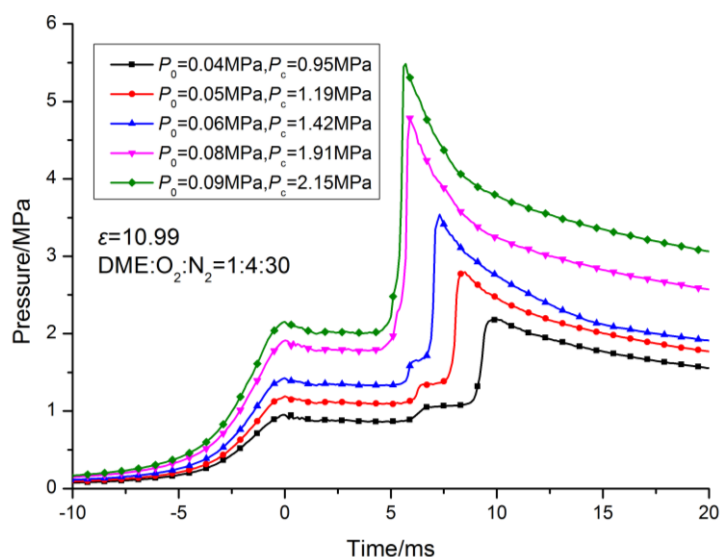

Figure 18. Effect of initial pressure on two-stage ignition delay ($\varepsilon = 10.99$).

4.5. Effect of Nitrogen Dilution Ratio on Two-Stage Ignition Delay

Figure 19 presents the test results with a nitrogen dilution ratio of 36.31%, 47.29%, 55.04%, and 60.81%. Inert gas is inactive in chemical reactions during the auto-ignition process. Physical parameters, such as specific heat at constant pressure, thermal conductivity, and thermal diffusivity, are the primary factors that influence the auto-ignition process. With the same compression ratio, the first-stage ignition delay shortens, whereas the second-stage ignition extends with increasing nitrogen dilution ratio (Figure 19). Considering that inert gas hinders the rise of auto-ignition pressure, the peak pressure of the DME–O_2–N_2 mixture decreases with increasing nitrogen dilution ratio. Figure 19a–f show the enlarged compressed pressure. With the same initial pressure and compression ratio, the increasing nitrogen dilution ratio leads to an increase in compressed pressure. The change of mixture composition by adding nitrogen alters the thermophysical properties of the DME–O_2–N_2 mixture, which might be one of the reasons why the first-stage ignition delay shortens. Adding nitrogen enhances the thermal capacity of the mixture, whereas the mole proportion of O_2 and DME is decreased. Consequently, the induction time before the high-temperature chemical reaction is prolonged. Similar to the influence of compression ratio on two-stage ignition delay, the test results on influences of nitrogen dilution ratio on two-stage ignition delay of the DME–O_2–N_2 mixture are summarized in three groups. Table 4 lists the overall ignition delay changing trends under various test conditions.

With a compression ratio of 8.82 and an initial pressure of 0.08 MPa (test condition group I), the first-stage ignition delay extends, whereas the second-stage ignition delay shortens. With increasing nitrogen dilution ratio, the first-stage ignition delay greatly shortens and the second-stage ignition delay gradually extends. Hence, the overall ignition delay tends to shorten.
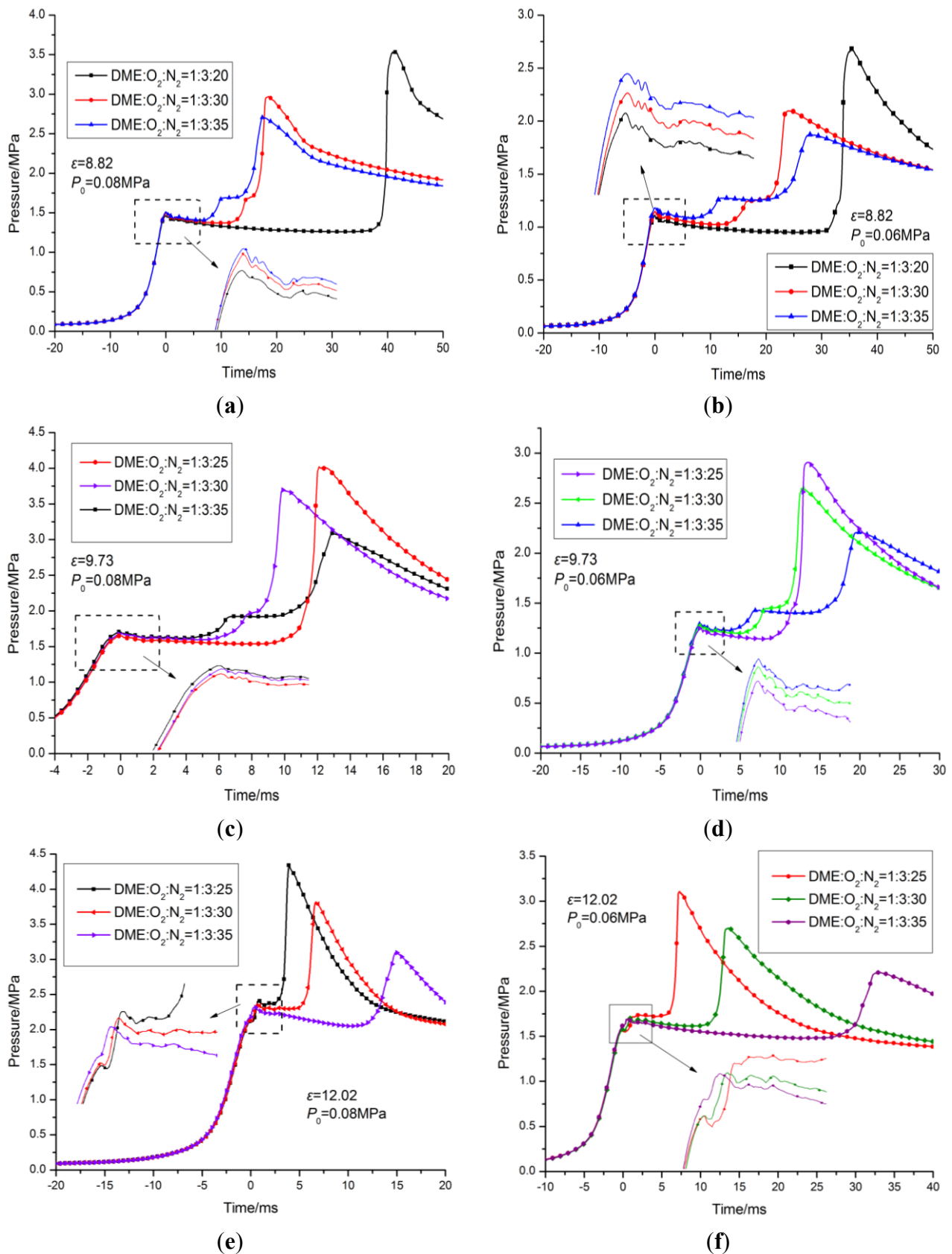
Comparatively, with a compression ratio of 12.02 and initial pressures of 0.06 MPa and 0.08 MPa (test condition group III), the first-stage ignition delay shortens, whereas the second-stage ignition delay extends. With increasing nitrogen dilution ratio, the first-stage ignition delay insignificantly shortens, whereas the second-stage ignition delay significantly extends. Thus, the overall ignition delay of the mixture tends to extend. Under the rest test conditions (test condition group II), in light of the different changes in the two-stage ignition delay, the overall ignition delay initially shortens and then extends.

In general, the overall ignition delay of the DME–O_2–N_2 mixture presents various changing trends with increasing nitrogen dilution ratio.

Table 4. Overall ignition delay changing trends with increasing nitrogen dilution ratio.

Test Condition Group	Test Condition	Changing Trend
I	$\varepsilon = 8.82$, $P_0 = 0.08$ MPa	Gradually shortens
II	$\varepsilon = 8.82$, $P_0 = 0.06$ MPa	Initially shortens and then extends
	$\varepsilon = 9.73$, $P_0 = 0.08$ MPa	
	$\varepsilon = 9.73$, $P_0 = 0.06$ MPa	
III	$\varepsilon = 12.02$, $P_0 = 0.08$ MPa	Gradually extends
	$\varepsilon = 12.02$, $P_0 = 0.06$ MPa	

Figure 19. Effect of nitrogen dilution ratio on two-stage ignition delay: (**a**) ε = 8.82, P_0 = 0.08 MPa; (**b**) ε = 8.82, P_0 = 0.06 MPa; (**c**) ε = 9.73, P_0 = 0.08 MPa; (**d**) ε = 9.73, P_0 = 0.06 MPa; (**e**) ε = 12.02, P_0 = 0.08 MPa; and (**f**) ε = 12.02, P_0 = 0.06 MPa.

5. Conclusions

A RCM test bench is developed in this study. Performance characterization tests and auto-ignition performance tests are carried out.

In the compression performance tests of the RCM, the effects of hydraulic buffer and driving gas pressure on the performance characterization are studied. The hydraulic piston with T-shaped channels is used to address the problem wherein the hydraulic buffer has an adverse impact on the compression process.

In the auto-ignition performance tests of the RCM, the effects of the driving gas pressure, compression ratio, initial pressure, and nitrogen dilution ratio on the two-stage ignition delay are studied. The drawn conclusions are as follows:

(1) With increasing driving gas pressure, both the first-stage and the overall ignition delays tend to increase. This result might be based on the fact that the $DME-O_2-N_2$ mixture has a low auto-ignition temperature. With low driving gas pressure and piston motion speed, the $DME-O_2-N_2$ mixture is much more strongly influenced by compression time. With high driving gas pressure and piston motion speed, the mixture is less influenced by the compression time. The driving gas pressure within a certain range insignificantly influences the compressed pressure.

(2) With increasing compression ratio, the compressed temperature rises and the first-stage ignition delay of the $DME-O_2-N_2$ mixture shortens, whereas the ignition delay of the second-stage extends. Under the various test condition groups, the overall ignition delay presents different trends: gradually shorten, then gradually extend, and initially shorten and then extend. This result can be attributed to the fact that the NTC region of the overall ignition delay of the $DME-O_2-N_2$ mixture changes with nitrogen dilution ratios and compressed pressure conditions.

(3) With the increasing initial pressure, both the first-stage and the second-stage ignition delays shorten. The second-stage ignition delay shortens to a greater extent than that of the first-stage. Compared with a lower compression ratio, the overall ignition delay of the $DME-O_2-N_2$ mixture under a high compression ratio shortens to a greater extent.

(4) With the increasing nitrogen dilution ratio, the first-stage ignition delay shortens, whereas the ignition delay of the second-stage extends. The increasing nitrogen dilution ratio leads to an increase in compressed pressure. The overall ignition delay of the $DME-O_2-N_2$ mixture presents different trends: gradually shorten, then gradually extend, and initially shorten and then extend.

Author Contributions

Hao Liu wrote the main part of the paper. Hongguang Zhang revised the paper. Zhicheng Shi, Haitao Lu, and Guangyao Zhao performed the experiments. Baofeng Yao participated in the RCM test bench design. All authors read and approved the manuscript.

Nomenclature

P_0 initial pressure [MPa]
P_c compressed pressure [MPa]
P_{drive} driving gas pressure [MPa]
T_0 initial temperature [K]
T_c compressed temperature [K]

Greek letters

γ   ratio of specific heat
ε   compression ratio

Acronyms

HCCI   homogeneous charge compression ignition
RCM   rapid compression machine
RCEM   rapid compression and expansion machine
NTC   negative temperature coefficient
TDC   top dead center
BDC   bottom dead center

Conflict of Interest

The authors declare no conflict of interest.

References

1. Sung, C.-J.; Curran, H.J. Using rapid compression machines for chemical kinetics studies. *Prog. Energy Combust. Sci.* **2014**, *44*, 1–18.
2. Mittal, G.; Sung, C.-J. Aerodynamics inside a rapid compression machine. *Combust. Flame* **2006**, *145*, 160–180.
3. Di Sante, R. Measurements of the auto-ignition of *n*-heptane/toluene mixtures using a rapid compression machine. *Combust. Flame* **2012**, *159*, 55–63.
4. Allen, C.; Mittal, G.; Sung, C.-J.; Toulson, E.; Lee, T. An aerosol rapid compression machine for studying energetic-nanoparticle-enhanced combustion of liquid fuels. *Proc. Combust. Inst.* **2011**, *33*, 3367–3374.

5. Gupta, S.B.; Bihari, B.; Sekar, R.; Klett, G.M.; Ghaffarpour, M. Ignition characteristics of methane-air mixtures at elevated temperatures and pressures. *SAE Tech. Pap.* **2005**, *2005*, doi:10.4271/2005-01-2189.

6. Lim, O.T.; Iida, N. The investigation about the effects of thermal stratification in combustion chamber on HCCI combustion fueled with DME/*n*-Butane using Rapid Compression Machine. *Exp. Therm. Fluid Sci*. **2012**, *39*, 123–133.

7. Katsumata, M.; Morikawa, K.; Tanabe, M. Behavior of shock wave and pressure wave of SI knocking with super rapid compression machine. *SAE Tech. Pap.* **2011**, *2011*, doi:10.4271/2011-01-1875.

8. Kobashi, Y.; Tanaka, D.; Maruko, T.; Kato, S.; Kishiura, M.; Senda, J. Effects of mixedness and ignition timings on PCCI combustion with a dual fuel operation. *SAE Tech. Pap*. **2011**, *2011*, doi:10.4271/2011-01-1768.

9. Guang, H.; Yang, Z.; Huang, Z.; Lu, X. Experimental study of *n*-heptane ignition delay with carbon dioxide addition in a rapid compression machine under low-temperature conditions. *Chin. Sci. Bull*. **2012**, *57*, 3953–3960.

10. Araki, M.; Dong, H.; Obokata, T.; Shiga, S.; Lshima, T.; Aoki, K. Characteristics of CNG direct injection with auto-ignition. *SAE Tech. Pap.* **2005**, *2005*, doi:10.4271/2005-26-358.

11. Monteiro, E.; Sotton, J.; Bellenoue, M.; Moreira, N.A.; Malheiro, S. Experimental study of syngas combustion at engine-like conditions in a rapid compression machine. *Exp. Therm. Fluid Sci*. **2011**, *35*, 1473–1479.

12. Murase, E.; Hanada, K. Control of the start of HCCI combustion by pulsed flame jet. *SAE Tech. Pap.* **2002**, *2002*, doi:10.4271/2002-01-2867.

13. Guibert, P.; Keromnes, A.; Legros, G. Development of a turbulence controlled rapid compression machine for HCCI combustion. *SAE Tech. Pap.* **2007**, *2007*, doi:10.4271/2007-01-1869.

14. Donovan, M.T.; He, X.; Zigler, B.T.; Palmer, T.R.; Wooldridge, M.S.; Atreya, A. Demonstration of a free-piston rapid compression facility for the study of high temperature combustion phenomena. *Combust. Flame* **2004**, *137*, 351–365.

15. Kee, S.-S.; Shioji, M.; Mohammadi, A.; Niishi, M.; Inoue, Y. Knock Characteristics and their control with hydrogen injection using a rapid compression/expansion machine. *SAE Tech. Pap.* **2007**, *2007*, doi:10.4271/2007-01-1829.

16. Kikusato, A.; Fukasawa, H.; Nomura, K.; Kusaka, J.; Daisho, Y. A study on the characteristics of natural gas combustion at a high compression ratio by using a rapid compression and expansion Machine. *SAE Tech. Pap.* **2012**, *2012*, doi:10.4271/2012-01-1651.

17. Cho, G.; Jeong, D.; Moon, G.; Bae, C. Controlled auto-ignition characteristics of methane-air mixture in a rapid intake compression and expansion machine. *Energy* **2010**, *35*, 4184–4191.

18. Pöschl, M.; Sattelmayer, T. Influence of temperature inhomogeneities on knocking combustion. *Combust. Flame* **2008**, *153*, 562–573.

19. Goldsborough, S.S. A crevice blow-by model for a Rapid Compression Expansion Machine used for chemical kinetic (HCCI) studies. *SAE Tech. Pap.* **2007**, *2007*, doi:10.4271/2007-01-1052.

20. Pan, L.; Hu, E.; Zhang, J.; Zhang, Z.; Huang, Z. Experimental and kinetic study on ignition delay times of DME/H_2/O_2/Ar mixtures. *Combust. Flame* **2014**, *161*, 735–747.

21. Yang, Z.; Wang, Y.; Yang, X.; Qian, Y.; Lu, X.; Huang, Z. Autoignition of butanol isomers/*n*-heptane blend fuels on a rapid compression machine in $N_2/O_2/Ar$ mixtures. *Sci. China* **2013**, *57*, 461–470.

22. Würmel, J.; Silke, E.J.; Curran, H.J.; Ó Conaire, M.S.; Simmie, J.M. The effect of diluent gases on ignition delay times in the shock tube and in the rapid compression machine. *Combust. Flame* **2007**, *151*, 289–302.

23. Ihme, M. On the role of turbulence and compositional fluctuations in rapid compression machines: Autoignition of syngas mixtures. *Combust. Flame* **2012**, *159*, 1592–1604.

24. Toulson, E.; Allen, C.M.; Miller, D.J.; Schock, H.J.; Lee, T. Optimization of a multi-step model for the auto-ignition of dimethyl ether in a rapid compression machine. *Energy Fuels* **2010**, *24*, 3510–3516.

25. Mittal, G.; Chaos, M.; Sung, C.J.; Dryer, F.L. Dimethyl ether autoignition in a rapid compression machine: Experiments and chemical kinetic modeling. *Fuel Process. Technol.* **2008**, *89*, 1244–1254.

26. Pyun, S.H.; Ren, W.; Lam, K.-Y. Shock tube measurements of methane, ethylene and carbon monoxide time-histories in DME pyrolysis. *Combust. Flame* **2013**, *160*, 747–754.

27. Yu, Y.; Vanhove, G.; Griffiths, J.F.; De Ferrières, S.; Pauwels, J.-F. Influence of EGR and syngas components on the autoignition of natural gas in a rapid compression machine: A detailed experimental study. *Energy Fuels* **2013**, *27*, 3988–3996.